Theory of Magnetic Properties of Actinide Compounds. I

J. M. Robinson* and Paul Erdös
Department of Physics, The Florida State University, Tallahassee, Florida 32306
(Received 29 March 1973)

UP, UAs, NpC, and crystals of other actinide compounds have metallic conductivity and are magnetically ordered. They exhibit discontinuous changes in the magnetic moment per actinide ion as a function of temperature. These are accompanied by large changes of the specific heat, magnetic susceptibility, and electrical conductivity, as well as in some cases by changes in the magnetic symmetry. The transition at the Néel temperature may also be of first order. A theory is developed that explains these phenomena quantitatively. Abandoning the concept of a specific configuration (valency) of the actinide ion, we show that the transition $5f^n \rightarrow 5f^{n-1}(6d\text{-}7s)^1$ occurs for a certain fraction of the ions at different temperatures. The transition is induced by the combined effect of a small energy gap (or overlap) between the $5f$ localized and $6d\text{-}7s$ band states, the shielded and therefore short-range Coulomb interaction between band and localized electrons, and the variation of the exchange interaction between ions with the occupation of the band. The free energy is miminized with respect to the occupation numbers of the band states and of the magnetic sublevels of the ions in the two different configurations. This yields the temperature dependence of the band occupation and sublattice magnetization. The other observables are calculated from these quantities and fit the experimental data well.

I. INTRODUCTION

The metallic compounds of actinide (A) elements with elements of group V and VI of the Periodic Table exhibit a wide variety of unexplained first-order magnetic and electronic phase transitions, a preliminary theory of which was presented previously.[1] The experimental data[2-5] of Figs. 6, 7, and 12 are typical examples.

First examine the temperature dependence of the relative ordered moment per U ion of the antiferromagnet UP (Fig. 6). As the temperature T is increased from 0 °K, the moment drops sharply by about 10% at $T' = 22.5$ °K (see Fig. 6).[3] There is no change at T' in the AFM-I-type ordering[5] defined in Fig. 1.

Next, looking at the relative ordered moment per Np ion in NpC, one observes[4] a moment drop at $T_C \cong 220$ °K (see Fig. 12). At this temperature, the ferromagnetic (FM) ordering transforms to the AFM-I-type structure.

The following characteristics are common to many metallic binary and ternary compounds of actinides with group-IV, -V, and -VI elements.

(i) The spatial ordering is of NaCl type.

(ii) The (presumably) first-order magnetic transitions are not accompanied by detectable changes in lattice structure or volume.[4,6]

(iii) The magnetic ordering is of the type FM, AFM-I, AFM-IA (see Fig. 1), or of intermediate type.[1,4,5]

(iv) The sublattice magnetization as a function of temperature does not in general follow a Brillouin-type curve, particularly in the neighborhood of the Néel temperature T_N (see Figs. 6 and 12).

(v) "Moment-jump" transitions may occur at T_N and also at lower temperatures T'.

(vi) The moment-jump transition is, in some but definitely not all cases, accompanied by a change in the type of magnetic ordering.

(vii) The magnetic powder susceptibility[7] usually increases steeply by a factor of about 2 at the transitions at $T = T'$ and $T = T_N$.

(viii) The moment-jump transition is accompanied by a sudden increase in resitivity ρ,[8] shown in Fig. 12. The usual change in ρ at T_N is observed for these compounds as well.

As a further example we mention UAs. This

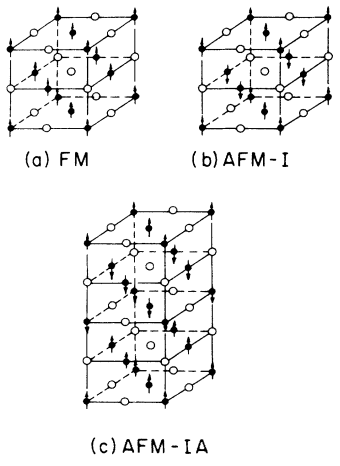

FIG. 1. Three types of magnetic order found experimentally in the NaCl-type metallic actinide compounds. The dots are the actinide ions, with the directions of their magnetic moments indicated by the arrows. The circles represent anions. (a) Ferromagnetic (FM). (b) Antiferromagnetic type I (AFM-I). (c) Antiferromagnetic type IA (AFM-IA).

TABLE I. Physical properties of selected NaCl-type metallic actinide compounds. a_0 is the lattice constant. The types of magnetic order found with increasing temperature are listed under "Order" and are defined in Fig. 1. T_t is a magnetic transition temperature; μ_0 is the ordered moment per A ion at $T=0\,^\circ$K; μ_p is the paramagnetic moment ; Θ is the Curie-Weiss constant; ρ is the resistivity at $T\simeq 200\,^\circ$K; γ is the band electronic specific heat coefficient.

AX	a_0(Å)	Order	T_t(°K)	$\mu_0(\mu_B)$	$\mu_p(\mu_B)$	Θ(°K)	$\rho(\mu\Omega$ cm)	$\gamma\ 10^{-4}\ \frac{\text{cal}}{\text{mole °K}^2}$	Refs.
UAs	5.779	AFM-I, -IA	66;127	2.24	3.54	32	238	?	a,b
UN	4.890	AFM-I	50	0.75	3.11	−325	160	96	b
USb	6.191	AFM-I	246	2.64	3.85	95	357	?	b,c
UP	5.589	AFM-I	22.5;121	1.95	3.15	00	370	23	d
US	5.489	FM	180	1.2−1.6	2.25	185	328	49	b
NpC	4.992	FM;AFM-I	220;310	2.1	3.22	225	200	?	e
NpSb	?	AFM	205	?	2.3	?	?	?	f

[a]Reference 9.
[b]Reference 32 and references cited therein.
[c]C. E. Olsen and W. C. Koehler, J. Appl. Phys. 40, 1135 (1969).
[d]References 7 and 2.
[e]References 4, 8, and 33.
[f]Reference 8.

compound will be treated in a forthcoming publication by the present authors (henceforth referred to as II). It should suffice to point out here the similarity of the dependence of its ordered moment[9,10] and of its magnetic susceptibility[11] to that of UP. A difference is that while UP does not change magnetic ordering at $T'=22.5\,^\circ$K, UAs changes from AFM-IA-type ($T<63\,^\circ$K) to AFM-I-type structure (see Fig. 1) at its moment-jump transition temperature $T'=63\,^\circ$K.[9,10] Other physical properties of these compounds are summarized in Table I.

Previous theories[12–14] have assumed a well-defined integral number of magnetic $5f$ electrons localized on each actinide ion. The ion, in turn, was assumed to be located in the customary "crystal field." These theories have not conclusively established the mechanism of the first-order transitions (except perhaps for the insulating compound UO_2[13]) since magnetization and susceptibility data were not simultaneously accounted for.

Furthermore, much recent experimental evidence[15–24] as well as calculations[25] indicate that at least some of the energy levels of the $5f$ electrons primarily responsible for the magnetic properties overlap those of the itinerant $6d$-$7s$ band electrons, as Fig. 2 shows. Given this overlap, one expects a temperature dependent distribution of electrons between f levels and the conduction band; i.e., the thermal average number of f electrons per ion will be a function of temperature. Not only will this effect be taken into account in the theory here described, but it will prove to be the decisive factor in explaining the phenomena listed in (i)–(viii).

Let us review some of the experimental evidence for the closeness or overlap of the $5f$ and $6d$-$7s$ levels, and for the resulting temperature dependence of the average number of f electrons per A ion.

The proximity of the Fermi level to the energy of the narrow $5f$-$6d$ band correlates well with the high values of the low-temperature electronic specific heat γ listed in Table I. (For comparison, $\gamma\cong 3.3\times10^{-4}$ cal/mole °K^2 for sodium metal.[26]) This effect has been connected with the observed temperature dependence of galvanomagnetic measurements on US,[15,16] PuC, PuP, and PuS.[17]

More recently, the anomalous maxima of the resistivity as a function of temperature found in Pu, Np, and $PuAl_2$ have also been explained[19] as resulting from the existence of both localized and itinerant states for the $5f$ electrons. For $T>100\,^\circ$K, the $5f$ electrons in these materials are thought to occupy mostly localized or "virtually bound" states. At lower temperatures, these electrons occupy itinerant bandlike states.[19]

The experiments of Matthias[20] have shown that the $5f$ electron can also be easily delocalized by the application of pressure on ferromagnetic and superconducting uranium compounds.

Sharp maxima in the electronic specific heat and electrical resistivity as functions of composition x of the solid solutions $UP_{1-x}S_x$[21] and $U_xTh_{1-x}S$[16] have been observed. Fisk and Coles[22] explained these maxima as resulting from the proximity in energy of virtually bound f levels to the Fermi surface of

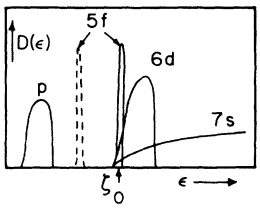

FIG. 2. Schematic representation of electronic density of states $D(\epsilon)$ as a function of electronic energy ϵ proposed for NaCl-type metallic actinide compounds. The Fermi level is denoted by ζ_0. Solid lines: after a calculation of Davis (Ref. 25); dashed lines: location of $5f$ levels, according to Grunzweig-Genossar *et al.* (Ref. 32).

the band states.

The observations showing the "lability"[20] or instability of the electronic configuration of the actinide ions cast serious doubt on the validity of the crystal field approach of previous theories. In Sec. II, a new model is proposed and the physical cause of the moment-jump transitions in the magnetically ordered state is explained as a partial delocalization of $5f$ electrons with decreasing temperature. In Sec. III, the mathematical details of the theory are developed. The model is specialized to the metallic actinide compounds in Sec. IV, followed by quantitative applications to UP and NpC. In publication II further applications to UAs, US, and the solid solutions $UP_{1-x}S_x$, $UAs_{1-x}S_x$, and $UP_{1-x}As_x$ are made.

II. PHYSICAL ORIGIN OF DELOCALIZATION TRANSITION

The discussion of Sec. I suggests the following simple model of the electronic states in the metallic actinide compounds.

(a) There are itinerant electronic states described by band theory. Let $D(\epsilon)$ be the density of states of the band as a function of energy ϵ (see Fig. 3).

(b) There are highly correlated, localized electronic states derived from the $5f$ actinide orbitals and described for a given ionic configuration (e.g., $5f^2$) as crystal field states of the ion.

(c) Each of the actinide (A) ions may be in one of two possible configurations. In one configuration there are M f electrons localized on the A ion, where M is a positive integer; and in the other configuration there are $M-1$ f electrons on the A ion, one f electron having "jumped" to an unfilled band state.

(d) There is a Coulomb repulsion between a localized electron and a band electron. We adopt the reasoning of Falicov *et al.*,[27,28] according to which the interaction energy is G if the localized and band electrons are in the same atomic (or Wigner-Seitz) cell and zero otherwise.

As a purely illustrative example of how a system described by the above assumptions can undergo a first-order phase transition, let us consider the case $M=1$, so that we allow either one or no $5f$ electron to be attached to each of the N actinide ions. The energy of the corresponding localized level is taken to be Δ' above the bottom of the band (see Fig. 3). We assume for the moment that this level is nondegenerate (as would be the case if, for example, it were the lowest component of an exchange split magnetic multiplet in the ordered state). The number of localized f electrons in the solid is given by $N(1-p)$, where $p(0 \le p \le 1)$ is the time-averaged probability that an actinide ion has lost one f electron to the band. The quantity p is determined for a given temperature T by minimizing the free energy F of the solid, given by

$$F(p) = U(p) - TS(p) , \tag{1}$$

where U and S are the internal energy and entropy, respectively. The internal energy is given by

$$U(p) = U_b(p) + N(1-p)\Delta' + U_G(p) . \tag{2}$$

The first and second terms are the internal energies of the system of band and localized electrons, respectively; and $U_G(p)$ is the total repulsive Coulomb interaction energy between the band and localized electrons: The quantity $U_b(p)$ depends on the density of states $D(\epsilon)$ of the band, but we can determine the qualitative features of the thermodynamic behavior without specifying $D(\epsilon)$.

We consider the case $\zeta(1) > \Delta'$, where $\zeta(p)$ is the Fermi energy of the band at $T=0$ °K when occupied by Np electrons; and we assume for simplicity that $\zeta(0)=0$. We treat two situations.

1. G = 0 [Fig. 3(a)]

In this case, there is one physical solution of $\delta F = 0$, $\delta^2 F > 0$ at $T=0$ °K, and the corresponding value

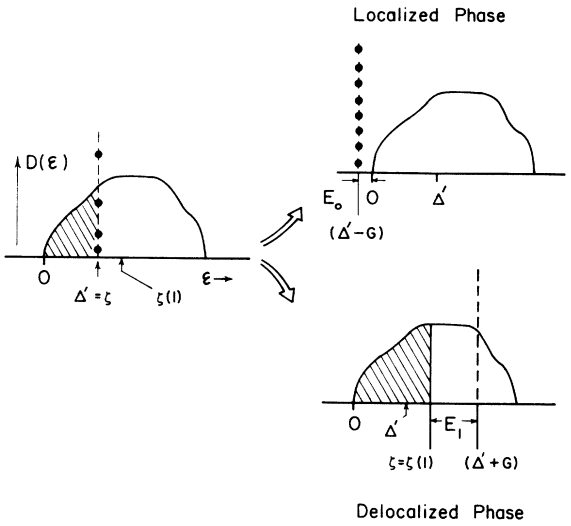

FIG. 3. Equilibrium distributions at $T=0$ °K of N electrons among N localized levels (vertical dashed lines) of energy Δ' and a band. $D(\epsilon)$ is the band density of states as a function of energy ϵ (continuous curve). The dots represent localized electrons, and the hatched regions are occupied band states. The short-range Coulomb interaction between band electrons and localized electrons is G, and ζ is the equilibrium Fermi level, which would equal $\zeta(1)$ if all N electrons were in the band. (a) If $G=0$, there is only one equilibrium electronic distribution, or phase. (b) If $G \ge \Delta'$, there are (as shown in the text) two possible stable equilibrium phases, called the localized and delocalized phases. The localized levels are shifted in energy by the Coulomb interaction, giving rise to the energy gaps E_0 and E_1 as shown.

of p is determined by the equation $\zeta(p)=\Delta'$, obtained from differentiating Eq. (2) with $U_G=0$ with respect to p and setting the result equal to zero. [Note that $dU_b(p)/dp=\zeta(p)$.] We see that the band is filled up to the energy Δ', and the remaining electrons occupy the localized levels. The minimum energy of a single particle excitation, in which either a band electron at the Fermi energy localizes or a localized electron "jumps" to a band state (i.e., "delocalizes") is zero in this case (there is no energy gap).

2. $G>0$ [Fig. 3(b)]

If G is finite, there may occur two solutions of $\delta F=0$, $\delta^2F>0$ as can be demonstrated by a simple argument. First, let us consider at $T=0$ °K a state with all the electrons localized ($p=0$), and calculate the energy E_0 required to excite a localized electron into the bottom of the empty band at $\epsilon=0$. In the band state the electron has a probability N^{-1} of being found in the Wigner-Seitz cell of any particular one of the $(N-1)$ actinide ions which are occupied by localized electrons. Thus the average value of the short-range Coulomb interaction in this state with one delocalized electron is $N^{-1}(N-1)G \cong G$. Since the solid loses the energy Δ' in transferring the electron to the bottom of the band, the result for E_0 is

$$E_0=G-\Delta' . \tag{3}$$

If the condition $E_0\geq 0$ holds, the localized state is stable with respect to single particle excitations and is therefore a possible physical solution of $\delta F=0$, $\delta^2F>0$.

Next, we imagine a state with all the electrons in the band ($p=1$) called the "delocalized" phase. The excitation of minimum energy is to bring one electron from the Fermi level [losing energy $\zeta(1)$] and localize it (gaining energy Δ'). Just as before, the Coulomb interaction between the localized and band electrons contributes G, so that we have

$$E_1=G+\Delta'-\zeta(1) . \tag{4}$$

If $E_1\geq 0$, the "delocalized" phase is also stable with respect to single particle excitations and is therefore also a possible physical solution of $\delta F=0$, $\delta^2F>0$ at $T=0$ °K.

In Fig. 3(b) the localized levels have been shifted in energy by the interaction G so as to give the correct excitation energies (3) and (4) with respect to the band. We now determine the conditions under which a first-order phase transition between the two phases is possible as T is increased from $T=0$ °K to $T=T'$. First, we assume that the internal energy $U(p=1)$ of the delocalized phase is lower than that of the localized phase at $T=0$ °K, so that the former phase is the physical ground state. This yields the condition

$$NE_g=U_b(1)-N\Delta'<0 , \tag{5}$$

where use has been made of the relation $U_G(0)=U_G(1)=0$. As T is increased, there arise thermal excitations of electrons across the gap E_1 [Fig. 3(b), lower diagram], resulting in a few electrons occupying localized states in the lattice of otherwise empty electron sites, or "holes." This increases the entropy S, because there are more microstates (or distinguishable distributions) corresponding to a lattice with two different kinds of ions than to a lattice of only one type of ion. If, however, there holds the condition

$$E_1\gg E_0 \tag{6}$$

the entropy of the metastable localized solution will rise much more rapidly as a function of T for $k_BT\simeq E_0$ than will the entropy of the delocalized ground state. The excitations in the latter phase will have their probabilities reduced by the Boltzmann factor e^{-E_1/k_BT}. Thus, the free energy $U-TS$ of the localized solution falls rapidly with increasing T and may cross below that of the delocalized phase at a finite temperature T', assuming that the initial separation E_g, given by Eq. (5), is smaller than k_BT'. At the temperature T' the system will undergo a first-order phase transition, the f electrons "condensing" from band or itinerant states into localized or ionic states. We have neglected here the excitation in which a band electron jumps from a state within or at the Fermi surface to an unoccupied band state. Because of the Pauli principle, these excitations play a negligible role as long as $K_BT'\ll\zeta(1)$.

For concreteness, we show that the conditions for the transition can be satisfied in the case of a parabolic dispersion curve $\epsilon_k\propto k^2$ for the band electrons. For this case, $U_b(1)=3N\zeta(1)/5$, and Eqs. (3)–(5) become

$$E_g=\tfrac{3}{5}\zeta(1)-\Delta', \tag{7}$$

$$E_1=G+\Delta'-\zeta(1) , \tag{8}$$

$$E_0=G-\Delta' . \tag{9}$$

A reasonable value for $\zeta(1)$ is 1.0 eV (or about 10^4 °K). For UP, $k_BT'\simeq 0.002$ eV, which we equate to E_g. From the discussion pertaining to Eq. (6) we assume $E_0=0$. Inserting these values into Eqs. (7)–(9), one finds $G=\Delta'=0.602$ eV and $E_1=0.204$ eV. Thus, the crucial condition $E_0\lesssim k_BT'\ll E_1$ is satisfied.

There is yet another mechanism which can lead to a first-order phase transition similar to that described above. If the localized level has a $(2J+1)$-fold magnetic degeneracy, the corresponding entropy $Nk_B\ln(2J+1)$ will favor a transition to the localized phase with increasing temperature. This mechanism is in fact the one proposed by Falicov

et al.[27] to explain the first-order α-γ phase transition observed in metallic cerium. However, it can hardly play a significant role at the moment-jump transitions of UP and UAs, because the exchange field in the magnetically ordered state lifts the degeneracy of the magnetic sublevels both before and after the transition. From the "flatness" of the magnetization versus T curves below and just above the transition at T' in UP and UAs one may also infer the absence of magnetic excitations near $T = T'$, which if present would decrease the magnetization smoothly with increasing T in each phase. The corresponding entropy of magnetic disorder is thus mostly suppressed and is apparently not the driving force for the moment-jump transitions. The transition discussed earlier in this section, in which the entropy of electronic excitations between localized and itinerant states plays the dominant role, is seen to have a fundamentally different origin from that proposed by Falicov *et al.*, even though it occurs within the framework of a similar model. An assumption of a small gap for localized-to-itinerant electronic transitions was also made by Nickerson *et al.*[29] in their theory of SmB_6, but they did not consider the Coulomb interaction G. That the entropy associated with electronic transitions between available states could be important at magnetic phase transitions was also suggested by Counsell *et al.*[18] as a result of their thermodynamic experiments on UN.

The main purpose of this section has been to show very qualitatively how the current view of narrow, mostly localized or "virtually bound" levels for the $5f$ electrons lying near the Fermi level of an overlapping band of itinerant electronic states can lead to first-order phase transitions, if the Coulomb interaction between electrons in the two types of states is taken into account. For the purposes of quantitative comparison to experiment, the model must clearly be generalized to include magnetic ordering and exchange interactions. This is done in Sec. III.

III. THEORETICAL MODEL

A. Hamiltonian and Assumptions of the Model

In generalizing the model of the previous section we begin with a Hamiltonian H, given by

$$H = \sum_{i=1}^{N} \sum_{q} \Delta_q L_i^{qq} + \sum_{\vec{k}} \epsilon_{\vec{k}} c_{\vec{k}}^{\dagger} c_{\vec{k}} + \sum_{i=1}^{N} \sum_{qt\vec{k}} \{ V_{i\vec{k}}^{qt} L_i^{qt} c_{\vec{k}}^{\dagger} + \text{H. c.} \}$$

$$+ \sum_{i\,qt} \sum_{\vec{k}\vec{k}'} U_{i\vec{k}\vec{k}'}^{qt} L_i^{qt} c_{\vec{k}'}^{\dagger} c_{\vec{k}} + H_{\text{mag}} \,. \qquad (10)$$

The quantities L_i^{qt} are the Hubbard-Haley[30,31] operators, which cause a transition of the actinide ion at site i from the state t to the state q. Note that the states q and t may differ in the number (n_q and n_t, respectively) of f electrons localized at the site. To each $n_j (n_j = 0, 1, 2, \ldots)$ there corresponds a set of discrete levels, obtained by the usual prescription of applying the crystal field of the surrounding ions as a perturbation on the states of the isolated actinide ion with n_j f electrons. The indices q and t in (10) run over all the levels resulting from considering each possible n_j. The operators $c_{\vec{k}}^{\dagger}$ and $c_{\vec{k}}$ are creation and destruction operators for the Bloch wave functions of the itinerant states. The third term is the hybridization between the localized and band electrons, the quantity $V_{i\vec{k}}^{qt}$ being a hopping matrix element for an ion in the state t at lattice site i to give up an electron to the band state $\vec{k}$ and go over to the ionic state q. The next to the last term in Eq. (10) is the Coulomb interaction between the band and localized electrons. The last term H_{mag} represents the exchange interactions coupling the actinide ions on different sites and in different magnetic sublevels and is discussed later. At this point, the following approximations (whose validity is discussed in Sec. IV) are made in the treatment of H.

(a) The "ionic" states q in the first term of Eq. (10) are restricted to those pairs of configurations which differ by unity in the number of localized electrons (e.g., in the case of UP these might reasonably be the $5f^2$ and $5f^3$ configurations.) The energies Δ_q of other configurations are assumed to be too large to be of physical interest.

(b) For each of the two configurations only the crystal field sublevel of lowest energy is considered. The configuration having M localized electrons (i.e., the "lower valent" state) is assumed to have an energy Δ_0, a magnetic degeneracy of $M_0 = 2s_0 + 1$, and a magnetic moment μ_0. The ionic state with $M-1$ localized electrons has energy Δ_1, degeneracy $M_1 = 2s_1 + 1$, and magnetic moment μ_1.

(c) The quantum-mechanical admixture of the band and localized states caused by the hybridization term in Eq. (10) is neglected.

(d) The Coulomb interaction between an ion and a band electron in a Wannier orbital centered on the site of the ion is G_0 if the ion has M localized electrons and G_1 if the ion has $M-1$ localized electrons. This is just a slight generalization of the short-range Coulomb interaction discussed in Sec. II. Furthermore, in what follows a Hartree approximation for this interaction is made, in which the operators $c_{\vec{k}'}^{\dagger}$, $c_{\vec{k}}$ and L_i^{qt} are replaced by their quantum statistical averages.

(e) The magnetic interactions H_{mag} are treated in the effective or molecular field approximation, in which a given magnetic ion interacts with an effective field $\lambda \vec{M}$ proportional to the sublattice magnetization $\vec{M}$. Only the magnetization due to the localized f electrons is considered; spin polarization of the itinerant electrons is neglected. The phenome-

nological coupling constant λ is allowed to depend on the occupation of the band and localized states and on the type of magnetic ordering, as discussed in Sec. IV.

B. Free Energy

We now derive the free energy $F = U - TS$ in terms of the occupation numbers of the localized and band states. The number of higher valent ions in the magnetic sublevel m_1 (m_1 ranges over the values $m_1 = -s_1, -s_1+1, \ldots, s_1$) is denoted by $\alpha(m_1)$, and the number of lower valent ions in the sublevel m_0 ($m_0 = -s_0, -s_0+1, \ldots, s_0$) by $\beta(m_0)$. The occupation of a band state of energy ϵ is $f(\epsilon)$. The occupation numbers are subject to the following constraints:

$$\sum_{m_1=-s_1}^{s_1} \alpha(m_1) = Np \,, \tag{11}$$

$$\sum_{m_0=-s_0}^{s_0} \beta(m_0) = N(1-p) \,, \tag{12}$$

$$\int_0^\infty D(\epsilon) f(\epsilon)\, d\epsilon = N(z+p) \,, \tag{13}$$

where zN (a constant for a given material) is the number of band electrons in the "localized" phase ($p = 0$).

First, we work out the internal energy U by taking the average value of the Hamiltonian Eq. (10) in a state with fixed values of the occupation numbers p, $\alpha(m_1)$, $\beta(m_0)$, and $f(\epsilon)$. Note that the neglect of hybridization and the approximate treatment of the Coulomb interaction mean that the original set of localized and band states are still eigenstates. In other words, an eigenfunction (or microstate) of the solid is written as the direct product of eigenfunctions $|q(i)\rangle$ of the ions, specified by giving the ionic state $q(i)$ of magnetic lattice site i, and of eigenfunctions $|\{n_{\vec{k}}\}\rangle$ of the electrons, specified by giving the occupation $n_{\vec{k}}$ ($n_{\vec{k}} = 0$ or 1) of every band state $\vec{k}$. The operators $c_{\vec{k}}^\dagger$ and L_i^{qt} operate independently on the band and ionic states, respectively. The ionic and band eigenfunctions are assumed to be orthonormal with respect to their quantum numbers. There are many microstates corresponding to given values of p, $\alpha(m_1)$, $\beta(m_0)$, and $f(\epsilon)$, but it will be seen that under our assumptions the internal energy U is independent of the particular microstate. An expectation value in a particular microstate is denoted by brackets ($\langle\rangle$).

The first term of Eq. (10) gives for the energy U_i of the localized electrons

$$U_i = \sum_q \Delta_q \sum_i \langle L_i^{qq} \rangle = N[\Delta_0(1-p) + \Delta_1 p] \,, \tag{14}$$

where assumptions (a) and (b) have been invoked. The second term of Eq. (10) yields the internal energy U_b of the band electrons

$$U_b = \sum_{\vec{k}} \epsilon_{\vec{k}} \langle c_{\vec{k}}^\dagger c_{\vec{k}} \rangle = \int_0^\infty \epsilon f(\epsilon) D(\epsilon)\, d\epsilon \,. \tag{15}$$

Only the diagonal terms $\vec{k} = \vec{k}'$ and $q = t$ are retained in the Coulomb interaction [fourth term in Eq. (10)]. The quantity $U_{i\vec{k}\vec{k}}^{qq}$ is the interaction energy between an ion at lattice site i in the state q and a band electron in the state $\vec{k}$. By assumption (d), this interaction equals $N^{-1} G_0$ if q corresponds to the $5f^3$ configuration and $N^{-1} G_1$ for the $5f^2$ configuration, independently of $\vec{k}$ and i.

The factor N^{-1} arises because an electron in a state with Bloch wave vector $\vec{k}$ has probability N^{-1} of being found in the atomic cell of the ion at site i. The expectation value U_G of the Coulomb interaction of the solid is then

$$\begin{aligned} U_G &= \sum_i \sum_q \langle L_i^{qq} \rangle\, U_i^{qq} \sum_{\vec{k}} \langle c_{\vec{k}}^\dagger c_{\vec{k}} \rangle \\ &= N[p(G_1/N) + (1-p)(G_0/N)]\, N(p+z) \,. \end{aligned} \tag{16}$$

The magnetic internal energy U_{mag} is (in the effective-field approximation) given by

$$U_{\text{mag}} = -\tfrac{1}{2} \lambda \vec{M}^2 = -\tfrac{1}{2} \lambda (N\mu/V)^2 \,, \tag{17}$$

where the moment μ per magnetic ion is written in terms of the magnetic occupation numbers as follows:

$$N\mu = \mu_1 \sum_{m=-s_1}^{s_1} m\alpha(m) + \mu_0 \sum_{m=-s_0}^{s_0} m\beta(m) \,. \tag{18}$$

We are assuming here that the symmetry of the magnetic lattice is sufficiently high so that the effective fields at the sites of the magnetic ions are equal in magnitude though not necessarily in sign, and therefore we do not need to introduce separate occupation numbers for each sublattice. This condition is satisfied for the FM, AFM-I and AFM-I*A* types of magnetic order (see Fig. 1) in the NaCl lattice. The internal energy U of the system is the sum of Eqs. (14)–(17).

The entropy S is calculated from the Boltzmann formula $S = k_B \ln W$, where W is the total number of microstates corresponding to fixed values of the occupation numbers p, $\alpha(m_1)$, $\beta(m_0)$, and $f(\epsilon)$. The entropy S_{ion} due to the ionic states is given by

$$S_{\text{ion}} = k_B \ln W_{\text{ion}} = k_B \ln N! \left(\prod_{m_0=-s_0}^{s_0} \beta(m_0)! \prod_{m_1=-s_1}^{s_1} \alpha(m_1)! \right)^{-1} . \tag{19}$$

The quantity W_{ion} is derived by calculating the total number of ways of distributing N distinguishable objects (the lattice sites) among $(2s_0+1)(2s_1+1)$ cells (the magnetic sublevels of the ions) such that the occupation numbers of the cells are specified by the $\alpha(m_1)$ and $\beta(m_0)$. The entropy S_b of the band electrons is given by the well-known expression[27]

$$S_b = -k_B \int_0^\infty D(\epsilon) \{ f(\epsilon) \ln f(\epsilon)$$

$$+[1-f(\epsilon)]\ln[1-f(\epsilon)]\}d\epsilon \ . \tag{20}$$

Taking into account the constraints (11)–(13) by introducing Lagrange multipliers ρ, τ, and λ, we can now write the free energy F as

$$\begin{aligned} F = {} & U_b - TS_b + N(1-p)\Delta - N(1-p)^2 G - \tfrac{1}{2}NJ\sigma^2 \\ & - TS_{\text{ion}} + \rho\Big(\sum_{m_1=-s_1}^{s_1}\alpha(m_1) - Np\Big) \\ & + \tau\Big(\sum_{m_0=-s_0}^{s_0}\beta(m_0) - N(1-p)\Big) \\ & + \zeta\,(zN + pN - \int_0^\infty D(\epsilon)f(\epsilon)d\epsilon) + K \ , \end{aligned} \tag{21}$$

where K [$K = \Delta_1 + (z+1)G_1$] is an unimportant constant. Here G, Δ, J, and σ are defined by the relations

$$G = G_0 - G_1 \ , \tag{22}$$

$$\Delta = \Delta_0 - \Delta_1 - G_0 + G(z+2) \ , \tag{23}$$

$$J = \lambda\,(N\mu_1/V)^2 \ , \tag{24}$$

$$\sigma = \mu/\mu_1 \ . \tag{25}$$

C. Magnetization and Band Occupation

Minimizing F with respect to $\alpha(m_1)$ and $\beta(m_0)$ yields the systems of equations

$$0 = \frac{\partial F}{\partial \alpha(m_1)} = -J\sigma m_1 + k_B T \ln\alpha(m_1) + \rho,$$

$$m_1 = -s_1, \ \ldots \ , \ s_1; \tag{26}$$

$$0 = \frac{\partial F}{\partial \beta(m_0)} = -Jr\sigma m_0 + k_B T \ln\beta(m_0) + \tau \ ,$$

$$m_0 = -s_0, \ \ldots \ , \ s_0 \ , \tag{27}$$

where $r = \mu_0/\mu_1$. From (26) and (27) one finds

$$\alpha(m_1) = e^{\beta(J\sigma m_1 - \rho)}, \ m_1 = -s_1, \ \ldots \ , \ s_1 \tag{28}$$

$$\beta(m_0) = e^{\beta(Jr\sigma m_0 - \tau)}, \ m_0 = -s_0, \ \ldots \ , \ s_0 \tag{29}$$

where $\beta = (k_B T)^{-1}$. Substituting Eqs. (28) and (29) into the constraint equations (11) and (12) yields

$$e^{-\beta\rho} = pZ_1^{-1}, \tag{30}$$

$$e^{-\beta\tau} = (1-p)\,Z_0^{-1} \ , \tag{31}$$

where

$$Z_1 = \sum_{l=-s_1}^{s_1} e^{\beta J\sigma l} \ , \tag{32}$$

$$Z_0 = \sum_{j=-s_0}^{s_0} e^{\beta Jr\sigma j} \ . \tag{33}$$

Now, inserting Eqs. (28)–(31) into Eq. (18), one obtains

$$\sigma = pB_{s_1}(x) + r(1-p)B_{s_0}(rx) \ , \tag{34}$$

where $x = \beta J\sigma$ and B_s is the Brillouin function. Setting the functional derivative of F [Eq. (21)] with respect to $f(\epsilon)$ equal to zero yields

$$f(\epsilon) = (e^{\beta(\epsilon-\zeta)} + 1)^{-1} \ , \tag{35}$$

where ζ is determined as a function of p and T by substituting (35) into the constraint equation (13):

$$\int_0^\infty D(\epsilon)\,(e^{\beta(\epsilon-\zeta)} + 1)^{-1}\,d\epsilon = N(z+p) \ . \tag{36}$$

Finally, minimizing F with respect to p gives the equation

$$\zeta - \Delta + 2G\,(1-p) - \tfrac{1}{2}\sigma^2\,dJ/dp + \tau - \rho = 0 \ . \tag{37}$$

Using Eqs. (30) and (31) one obtains from (37) the result

$$p^{-1} = 1 + Z_0\,Z_1^{-1} \exp\beta\,[\zeta(p) - \Delta + 2G\,(1-p) - \tfrac{1}{2}\sigma^2 J'(p)] \ , \tag{38}$$

where $J' = dJ/dp$. The three equations (34), (36), and (38) are three self-consistent equations in ζ, p, and σ for a fixed temperature T. The physical solution is that solution associated with the lowest free energy F [Eq. (21)]. The parameters of the theory are Δ, G, μ_1, r, $J(p)$, $D(\epsilon)$, and z and are characteristics of the substances under consideration. These parameters may be taken from experiment, calculated from another theory, or used as disposable fitting parameters.

D. Magnetic Susceptibility

The magnetic susceptibility χ of a powder sample of an antiferromagnet is written as

$$\chi = \tfrac{1}{3}\chi_{\parallel} + \tfrac{2}{3}\chi_{\perp} + \chi_{el} \ . \tag{39}$$

Here χ_{el} is the isotropic Pauli susceptibility of the band electrons, and $\chi_{\parallel}$ and $\chi_{\perp}$ are the susceptibilities of the localized $5f$ electrons for the test field h applied parallel and perpendicular, respectively, to the unique axis of the AFM-I or AFM-IA magnetic structures depicted in Fig. 1. The quantity $\chi_{\parallel}$ is defined by the expression

$$\chi_{\parallel} = \frac{N_A}{M}\,\mu_1 \lim_{h\to 0}\frac{\sigma^+(T) - \sigma^-(T)}{2h} \ , \tag{40}$$

where $N_A = 6.023\times 10^{23}$ and M is the gram-molecular weight of the sample. The terms σ^+ and σ^- are the magnitudes of the thermal average moments in units of μ_1 per ion of the sublattice whose moments are parallel or antiparallel, respectively, to the test field h. There should arise also a small difference δP in the time-averaged delocalization probability p for the two sublattices if $r < 1$. This is because the ions of the "up" sublattice can lower their interaction with the applied field h by ionizing to the state of higher magnetic moment, which is in this case the higher valent configuration. The resulting contribution $\sigma\delta p$ to the thermal average magnetization is expected to be small if the moments μ_0 and μ_1 of the two ionic configurations are

TABLE II. Parameters (in eV, except r, z, and m^*/m, which are dimensionless) of the electron delocalization theory of the magnetic actinide compounds UP and NpC used in fitting Figs. 6 and 12. Models A–F are explained in the text.

	UP			NpC		
	A	B	C	D	E	F
Δ	0.515	0.421		3.12	1.00	0.717
G	0.211	0.145		0.707	0.263	0.214
r	0.89	0.89	same as B	0.7	0.7	0.28
z	0.1	0.2		0.7	0.7	0.5
m^*/m	6.85	8.40		1.76	5.76	7.4
$J(0)$	0.018	0.025		0.043	0.047	0.017
$J_{FM}(0)$	0.0	0.0	0.011	···	···	···
$J_{FM}(1)$	−0.029	−0.020	same as B	···	···	···
$J'(0)$	···	−0.029		···	···	···
$J'_{FM}(0)$	···	···	−0.126	···	···	···
$J''_{FM}(0)$	···	···	0.255	···	···	···

nearly equal, i.e., if $r \cong 1.0$ as for UP (see discussion of Sec. IV and Table II) and UAs (see paper II). It is a useful simplification to neglect the influence of the test field on p, as an exact solution of the model of Sec. III in an applied field is quite difficult.

We first consider Eq. (34) (with $s_1 = 1$ and $s_0 = \frac{1}{2}$ as discussed in Sec. IV) for the average moment of the "up" sublattice, obtaining

$$\sigma^+(T) = pB_1(y) + r(1-p)B_{1/2}(yr), \tag{41}$$

where

$$y = \beta[\mu_1 h + J_1(p)\sigma^+ - J_2(p)\sigma^-]. \tag{42}$$

Here p is considered fixed at its thermal equilibrium value for $h = 0$. The exchange interaction $J(p)$ has been separated into its two components $J_1(p)$ and $-J_2(p)$, the former representing the interaction of an ion of one sublattice with all the ions of that same sublattice and the latter representing the interaction with the other sublattice in the AFM state. We next replace $\sigma^\pm$ in Eqs. (41) and (42) by $\sigma \pm d\sigma$, where σ is the equilibrium solution for the ordered moment in no applied field, and expand the resulting expression to first order in h and $d\sigma$. Substituting the result for $d\sigma$ into Eq. (40) yields

$$\chi_\parallel = N_A M^{-1} \mu_1^2 [J_{FM}(1-\phi)]^{-1}, \tag{43}$$

where

$$\phi = J_{FM}\beta\{r^2(1-p)[1-\tanh^2(rx)] + 3pZ_1^{-2} + pZ_1^{-1}\}, \tag{44}$$

$$J_{FM}(p) = J_1(p) + J_2(p). \tag{45}$$

The perpendicular susceptibility $\chi_\perp$ can be calculated by treating the thermal average magnetic moments as classical vectors[26] (note that there is no change in the magnitude of σ to first order in h), and one obtains

$$\chi_\perp = N_A M^{-1} \mu_1^2 [J(p) - J_{FM}(p)]^{-1}, \quad T \leq T_N$$

$$\chi_\perp = \chi_\parallel(\sigma = 0), \quad T > T_N. \tag{46}$$

The band susceptibility χ_{el} is given by[26]

$$\chi_{el} = N_A M^{-1} \mu_B^2 (z+p)^{1/3} [3\pi^2 (N/V)]^{-2/3} (2m^*/\hbar^2), \tag{47}$$

and is usually small compared to $\chi_\parallel$ or $\chi_\perp$.

Equations (39) and (43)–(47) are the desired results for the magnetic susceptibility χ in the special form implied by the model outlined in Sec. IV for the case $r \cong 1$. The quantity $J_{FM}(p)$ appearing in the above formulas is the $\vec{q} = 0$ (or FM) Fourier component of the exchange interaction, i.e., the interaction of a moment μ_1 with a lattice of similar moments all aligned parallel to the first. In the Ruderman-Kittel-Kasuya-Yosida (RKKY) calculation $J_{FM}(p)$ would correspond to the curve marked FM in Fig. 5. Note that $J_{FM}(p)$ does not arise in the theory of the magnetization in the AFM state, and is unknown if the RKKY theory is not valid for its prediction. In this case, there is no unique prediction for the susceptibility corresponding to a calculation of the magnetization in the ordered state, and the function $J_{FM}(p)$ must be parameterized in the same way as will be discussed in Sec. IV for the exchange $J(p)$ which occurs in Eqs. (34) and (38).

IV. APPLICATION OF THEORY TO UP AND NpC

A. Ionic Levels, Band Density of States, and Exchange Interactions

We now investigate the as yet unspecified ionic levels, band density of states $D(\epsilon)$, and magnetic exchange interaction $J(p)$ in the light of the known facts concerning UP, UAs, and NpC.

First, the two ionic configurations will be chosen to correspond to the $5f^2$ and $5f^3$ configurations of the actinide ions. This choice is primarily justified by the fact that the predicted paramagnetic moment μ_p for the lowest Russell-Saunders J multiplets of the $5f^3$ ($\mu_p = 3.61\mu_B$) and $5f^2$ ($\mu_p = 3.57\mu_B$) states are nearly equal and in good agreement with the experimental results for UP ($\mu_p = 3.45\mu_B$),[3] UAs ($\mu_p = 3.15 - 3.56\mu_B$),[32] and NpC ($\mu_p = 3.22\mu_B$).[33] The neutron diffraction work is also unable to definitely distinguish between the two configurations.[32,34] The lowest crystal field level of the $5f^3$ configuration is assumed to be the E_1' (or Γ_6) doublet ($s_0 = \frac{1}{2}$) with a magnetic moment μ_0. The $5f^2$ configuration, which characterizes all the ions in the delocalized phase at $T = 0\,^\circ$K, is treated as an F_{2g} (or Γ_5) magnetic triplet ($s_1 = 1$) having a theoretical moment $\mu_1 = 2.0\mu_B$ (see Fig. 4).[35] This agrees with the ordered magnetic moment μ_n at $T = 0\,^\circ$K deduced from neutron diffraction experiments on UP [$\mu_n = (1.95 \pm 0.05)\mu_B$],[36] UAs [$\mu_n = (2.2 \pm 0.05)\mu_B$],[37] and NpC [$\mu_n = (2.1 \pm 0.1)\mu_B$].[4] The above choices for the localized levels are not unique but are the simplest assumptions compatible

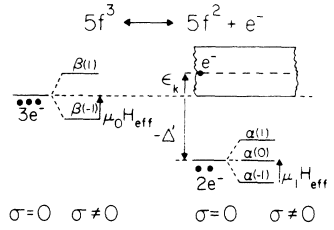

FIG. 4. Energy levels in the electron delocalization model of UP, UAs, and NpC. The symbols Δ, μ_0, μ_1, σ, $\alpha(m_1)$, $\beta(m_0)$ and ϵ_k are explained in the text, and H_{eff} is the molecular field, proportional to σ.

with the observed magnetic moments and the crystal symmetry in the metallic actinide compounds. We recall also from the discussion in Sec. II that the low-temperature moment-jump transition is not expected to depend much on the multiplicities of the magnetic manifolds, at least for UP and UAs. The parameter $r = \mu_0/\mu_1$ is allowed to vary within reasonable limits as crystal field theory is not completely reliable for its prediction (see Sec. VI B). The neglect of crystal field levels of higher energy also restricts us to low-temperature applications. For example, the paramagnetic susceptibility will not be treated under the present approximations.

Note that the localized "ionic" levels described above are here used as basic states, the occupation numbers of which determine thermodynamic properties in the mean-field approximation. Because of the neglect of the hybridization term in the Hamiltonian (10) these ionic states are not the exact electronic eigenstates of the solid. In fact, if the energies of the f electrons lie in the continuum of the band energies as shown in Figs. 2 and 3 there can be no truly bound or localized states.[38] If the hybridization is weak, however, electrons in the narrow f levels may be viewed as "virtually bound" in the sense of remaining on the actinide ion for a period which is very long compared to that of a band electron. In such a case, it is a reasonable approximation to treat the localized f levels for each configuration in the crystal field scheme as done here. This view of the f levels in the metallic NaCl-type actinide compounds was also proposed by Wedgwood[23,24] and by Fisk and Coles[22] as a result of their experiments. The assumption of a weak hybridization is also supported by the fact that the magnitudes ($\sim 2.0\mu_B$) of the ordered magnetic moments in UP, UAs, and NpC agree well with the predictions of the crystal field theory. As shown by Anderson[38] a strong hybridization would have the effect of reducing the local moment or eliminating it, as is believed to be the case for the lighter actinide metals.[39] The neglect of the magnetic moments of the itinerant electrons is also supported by the neutron diffraction experiment of Wedgwood[24] on monocrystalline US, in which only a small negative spin polarization of the $6d$ and $7s$ electrons was found in the ordered state.

Our assumptions are, however, not adequate for calculating quantities, such as electronic charge density, which are sensitively dependent upon the hybridization and the band structure. When an electron is "delocalized", its charge density probably remains mostly concentrated on the actinide lattice sites, because the band states are primarily derived from the $6d$ and $7s$ (and possibly even $5f$) actinide atomic orbitals. This is evidenced by the fact that no significant volume change at $T = T'$ is experimentally found for UP[6] or NpC.[4] That such changes need not necessarily accompany electron delocalization transitions is illustrated by the examples of Fe_3O_4,[40,41] Ti_2O_3,[42] and several rare-earth cobaltates ($RCoO_3$),[43,44] all of which exhibit first-order localized-to-itinerant electronic transitions with small ($\sim 0.1\%$) or unobservably small volume discontinuities.

The density of states $D(\epsilon)$ of the band is not known accurately for the actinide compounds. In all subsequent applications, we assume for simplicity a quadratic dispersion for the itinerant electrons:

$$\epsilon_{\vec{k}} = (\hbar^2/2m^*)\,k^2, \tag{48}$$

where m^* is the "effective mass." Now $D(\epsilon)$ becomes simply

$$D(\epsilon) = (V/2\pi^2)(2m^*/\hbar^2)^{3/2}\epsilon^{1/2}, \quad \epsilon > 0$$
$$= 0, \quad \epsilon \leq 0 \tag{49}$$

where no "cutoff" has been taken at high energy. The effects of such a cutoff should be negligible for partially filled bands ($\zeta > 0$) at the low temperatures ($T \lesssim 10^2\,^\circ\text{K}$) of interest here, because the distribution function $f(\epsilon)$ falls off exponentially for $\epsilon > \zeta$. For the same reasons, Eq. (36) may be solved for $\zeta(p)$ as follows:

$$\zeta(p) = \zeta_0(p)[1 - \tfrac{1}{12}\pi^2(k_BT/\zeta_0(p))^2 + \ldots], \tag{50}$$

where

$$\zeta_0(p) = (\hbar^2/2m^*)[3\pi^2(N/V)]^{2/3}(z+p)^{2/3}. \tag{51}$$

With Eq. (50) substituted for $\zeta(p)$, we have two self-consistent equations (34) and (38) to solve for σ and p. The free energy at equilibrium is now

$$F = F_b + N\Delta(1-p) + \tfrac{1}{2}NJ\sigma^2 - N(1-p)^2G$$
$$- Nk_BT\ln\{(Z_1/p)^p[(1-p)/Z_0]^{p-1}\}, \tag{52}$$

where

$$F_b = \tfrac{3}{5}N(z+p)\zeta_0(p)\{1 - \tfrac{5}{12}\pi^2[k_BT/\zeta_0(p)]^2 + \ldots\}. \tag{53}$$

The parameters of the model are now z, Δ, G,

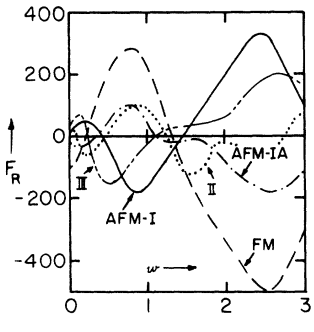

FIG. 5. RKKY exchange interaction energy F_R (in arbitrary units) of a magnetic ion at a given lattice site with all other magnetic ions in the NaCl lattice. F_R is plotted as a function of the number of conduction electrons w per magnetic ion and for various types of magnetic order. The types II and III (Ref. 32) are not observed experimentally in the actinide compounds. AFM-IA, this work; other curves, Ref. 32.

m^*/m, r, and $J(p)$.

The effective exchange interaction $J(p)$ is due to two sources in the metallic actinide compounds. One source is the (short-range) direct or superchange interactions between the localized $5f$ electrons of different actinide ions. This exchange is expected to depend upon the time-averaged number of localized $5f$ electrons and therefore upon p but should be independent of z. A second source of exchange is the indirect exchange, coupling localized moments via exchange with conduction electrons. In the RKKY[45] theory, the resulting effective exchange interaction J_{ij} between two magnetic ions i and j has the same form $J_{ij}\vec{S}_i \cdot \vec{S}_j$ as the direct or superexchange, but the coupling J_{ij} is of long range and depends on the occupation wN of the band (Here, $w = z + p$). The resulting interaction $F_R = \langle \sum_j J_{ij}\vec{S}_i \cdot \vec{S}_j \rangle$ is shown in Fig. 5 in arbitrary energy units as a function of the total band occupation wN for various types of magnetic orderings in the NaCl-type lattice.[32] If only this RKKY exchange were present, the magnetic ground state for a given value of w would be that type of order having the lowest energy in Fig. 5, and the p dependence of J and J' occurring in Eqs. (34) and (38) would be completely specified. The presence of direct exchange of comparable magnitude and the probable complexity of the actual band structure of the metallic actinides render the calculation which led to Fig. 5 of only qualitative significance. However, two very important conclusions may still be drawn from the inspection of the curves in Fig. 5.

(a) At an electron delocalization transition at $T = T'$ in the magnetically ordered state, where there is a discontinuous change in p, the type of magnetic order either changes (as observed for NpC and UAs), if the magnetic phases of lowest energy for the values of w above and below $T = T'$ are different, or does not change (example: UP), if the two phases are the same.

(b) The continuous increase of p with temperature above $T = T'$ in the localized phase (see Sec. II) will cause the exchange $J(p)$ in Eq. (34) to be temperature dependent, so that the resulting $\sigma(T)$ function for the sublattice magnetization will in general be a non-Brillouin curve. In particular if dJ/dp is large in magnitude and negative, $\sigma(T)$ is expected to fall steeply as T approaches T_N, as is observed in UP and UAs.

Thus, the magnetic exchange $J(p)$ provides the last element needed in our theory to explain all aspects of the magnetic transitions observed in UP, UAs, and NpC. The qualitative features of the calculation of Fig. 5 are in agreement with experiments on solid solutions $UP_{1-x}S_x$,[46-48] $UAs_{1-x}S_x$,[9] $UP_{1-x}As_x$,[10] and $UAs_{1-x}Se_x$,[49] where changes of the magnetic phase with x can be related to changes in the number of band electrons[47,48] (see also paper II).

A computer program was written which, for fixed values of the parameters z, Δ, G, m^*/m, and r and for any specified function $J(p)$, finds all of the solutions of Eqs. (34) and (38) at a particular temperature T. Each solution yields a pair of numbers for p and σ in the interval [0, 1], which is then substituted into Eq. (52) to find the solution of lowest free energy F for the given value of T.

B. Uranium Monophosphide (UP)

The experimental sublattice magnetization and powder susceptibility of UP are shown in Fig. 6.

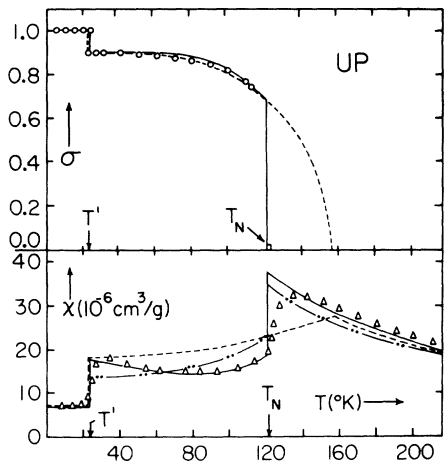

FIG. 6. Relative sublattice magnetization σ (top diagram) and magnetic powder susceptibility χ of UP as functions of temperature T. $T' = 22.5$ °K and $T_N = 121$ °K, in agreement with the data of Fig. 7. Top: Circles, NMR experiment of Carr *et al.*, Ref. 3; dashed curve, theory, with parameters from column A of Table II: solid curve, theory, with parameters from columns B or C of Table II. Bottom: triangles, experiment of Gulick and Moulton, Ref. 7; dashed curve, theory, column A of Table II; dash-dotted curve, theory, column B of Table II; solid curve, theory, column C of Table II.

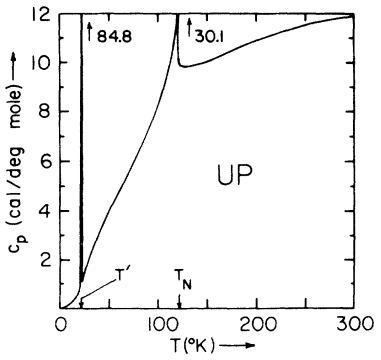

FIG. 7. The molar heat capacity c_p of UP as a function of temperature T according to the experiment of Counsell *et al.*[2] Note the unusually sharp singularities at $T' = 22.5$ °K and at $T_N = 121$ °K.

We note that the value for the Néel temperature is best determined from the data of Counsell *et al.*,[2] who find an almost vertical ascent of the specific heat c_p upon cooling to $T = T_N = 121$ °K (see Fig. 7). This determination of T_N is also consistent with the temperature of steepest descent of the magnetic susceptibility, as discussed in Ref. 7. The even more dramatic singularity in c_p at $T = 22.5$ °K also agrees very well with the NMR data of Ref. 7. The neutron diffraction data,[5,36] on the other hand, are less accurate for the exact determination of the transition temperatures. The details of the magnetization curve near $T = T_N$ cannot be ascertained from the experiments, but from examining the NMR data of Fig. 6 up to 115 °K it can be seen that the fall-off of the magnetization near T_N must be quite rapid if not discontinuous. Furthermore, from Fig. 7 it appears that most of the entropy of magnetic disordering is generated within 10–15 °K of the Néel temperature, also indicating a sharp transition.

Now let us estimate the values of the parameters m^*, z, r, G, Δ, and $J(p)$ appropriate for UP. Experiments on spin-disorder scattering[32] and low-temperature electronic heat capacity[2] suggest the range of values $m^*/m \simeq 5.0$–9.0 for the effective mass m^* (m = free electronic mass). The estimate $w_0 \simeq 1.05$ for the number of conduction electrons per U ion at $T = 0$ °K has been deduced from experiments[47,48] on solid solutions. From the condition that the AFM-I magnetic ordering be the magnetic phase of lowest energy the RKKY calculation (Fig. 5) requires $0.67 \leq w_0 \leq 1.33$. Since as discussed earlier we expect the ground state at $T = 0$ °K to be the delocalized phase for which $p = 1$, we have the result $w_0 = 1 + z$. From this and the preceding discussion we see that the range of values $z \simeq 0.0$–0.3 is reasonable for the parameter z. The quantity r can be calculated from crystal field theory, but the results depend on the details of the calculation. The values $r = 0.67$,[35] 0.85,[50] and 0.92[24] have been obtained. The Coulomb interaction G is not known for the actinide compounds. For the $4f$ electrons of Ce metal Ramirez and Falicov find $G = 0.44$ eV.[27] There is also no known estimate for Δ, but the conditions derived in Sec. II for a first-order transition allow it to be approximately determined, once G is specified.

It is instructive to first consider the case $J(p) = J$, a constant independent of p. Values for the remaining parameters compatible with the above estimates were selected as listed in Table II, column A, and the resulting reduced magnetization $\sigma(T)$ and susceptibility $\chi(T)$ are plotted in Fig. 6 (dashed curves). As expected, the magnetization does not fall off sharply enough near $T = T_N$, but the moment-jump transition at $T = T'$ is very well explained. The internal energy U, the quantity $-TS$ (S = entropy) and the free energy F are shown as functions of p for two values of T in Fig. 8. There are two minima in $F(p)$, indicating two possible physical phases, and the transition results from a shift in the absolute minimum from $p \cong 1.0$ for $T < T'$ to $p \cong 0.0$ for $T > T'$. The free energy F as a function of T for the two phases in Fig. 9 shows the transition at $T = T'$. The corresponding contributions $-TS$ of the entropy S of magnetic and electronic excitations to the free energy F are shown in Fig. 10. It is seen that the analysis of Sec. II is confirmed in that the entropy of thermally created holes in the localized phase is the main "driving force" for the transition at $T = T'$. The behavior of the band occupation $w = z + p$ as a function of T (Fig. 11) shows that only values of p near $p = 1$ and $p = 0$ physically occur for $T < T_N$ and suggests a convenient approximation for taking into account the important p-dependence of the exchange $J(p)$:

$$J(p) = J(1), \qquad p \cong 1$$
$$= J(0) + J'(0)p + J''(0)p^2, \quad p \ll 1 \ . \tag{54}$$

In the calculation of Fig. 6 (solid curve), the number of additional parameters so introduced was reduced to one [$J'(0)$] by the assumptions $J(1) = J(0)$ and $J''(0) = 0$. In this way, good agreement between the experimental and theoretical magnetization curves was finally obtained. The ferromagnetic component $J_{FM}(p)$ of the exchange needed for the susceptibility derived in Sec. V was also written as in Eq. (54), and the assumptions $J'_{FM}(0) = J''_{FM}(0) = 0$ were made in the calculations of Fig. 6(b) (Table II, columns A and B). It was necessary to invoke the full variational freedom of Eq. (54) for $J_{FM}(p)$ to obtain the good agreement shown by the solid line in Fig. 6(b) (see Table II, column C). In these models, the sharp increase in the exchange $J_{FM}(p)$

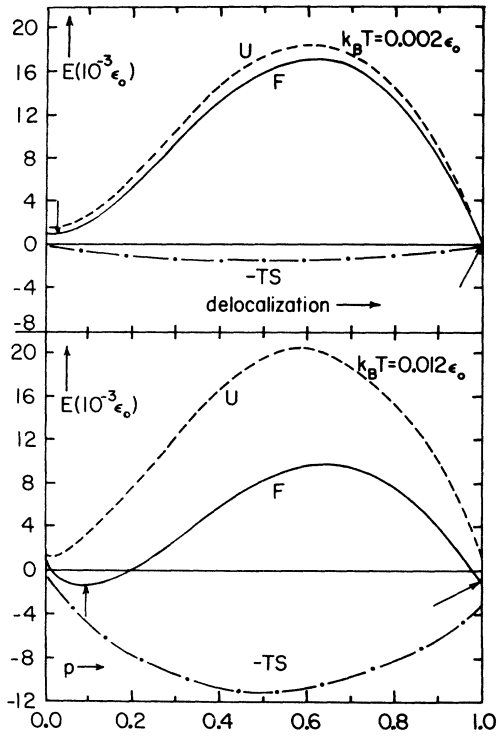

FIG. 8. The internal energy U, the quantity $-TS$ (S = entropy) and free energy F of UP for the parameters of Table II, column A as functions of the delocalization parameter p for two different temperatures T. $z+p$ is the average number of band electrons per actinide ion, where $z=0.1$. For each value of p, the renormalized magnetization σ is taken from that solution of Eq. (34) which has the lowest free energy. The unlabeled arrows indicate minima in the function F. The absolute minimum shifts from $p \cong 1.0$ at low T (upper drawing) to $p \cong 0.1$ at higher T (lower drawing), indicating a first-order transition at some intermediate temperature. The Fermi-energy when there is 1 electron per U atom in the band is $\epsilon_0 = 0.444$ eV.

as T is lowered below the transition at $T=T'$ is primarily responsible for the observed sharp decline of $\chi(T)$. That such a change in $J(p)$ is not unreasonable is seen from Fig. 5.

We note that the minimum value of $w=z+p$ occurring in the best fit (models B or C) is $w \simeq 0.25$, outside the regime of the AFM-I ordering calculated by the RKKY theory, which thus wrongly predicts a change in the spin structure at $T=T'$. However, the presence of competing antiferromagnetic direct exchange or superexchange could broaden the region of stability of the AFM-I phase, as is discussed in Sec. IV.

The predictions of models A and B (or C) for the heat of transition $T\Delta S$ of the transitions at $T=T'$ and $T=T_N$ and the low-temperature ($T<T'$) electronic specific heat are compared to the experiment of Counsell *et al.*[2] in Table III and good agreement is found in the case of the latter model. Note that because the theory of model A is not adequate near $T=T_N$, there is no entry for $T\Delta S$ at $T=T_N$ for this model.

Quite recently, Troc[11] sent us some preliminary unpublished experimental data on arcmelted samples of UP which show a sudden increase in the electrical resistivity $\rho(T)$ on heating through the transition at $T=T'$. These data lend further support to the model herein presented.

C. Neptunium Monocarbide (NpC)

The compound NpC exists only as a NaCl-type "defect structure" (i.e., having vacancies at some carbon sites)[4] described by NpC_x, where values of x from $x=0.82$ to $x=0.96$ are experimentally realized.[8] The Néel temperature is strongly dependent on x but not the FM–AFM-I transition temperature T'.[8] In the present theory of the data of Fig. 12, the effects of the carbon vacancies are not explicitly considered. No experiments concerning z, m^*, the electronic specific heat, or the heats of transition are known to the authors at present, so that widely differing sets of parameters provide reasonable "fits" to the data. Three such parameter sets (models D, E, and F) are listed in Table II and the corresponding predictions for the renormalized sublattice magnetization $\sigma(T)$ and the band occupation $w(T)$ are displayed in Fig. 12. In the first two models (columns D and E of Table II) the p dependence of $J(p)$ is neglected (as in model A for UP, Table II), and in the third model (column F of Table II) the RKKY calculation is used for $J(p)$. Comparing the values of $w(T)$ for T just below and just above $T=T'=220$ °K to the RKKY calculation of Fig. 5, we see that the latter theory

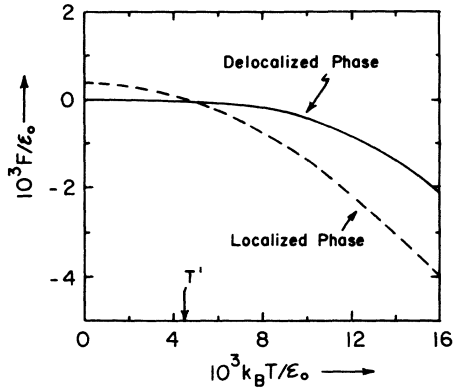

FIG. 9. The free energy F as a function of temperature T for the localized (dashed curve) and delocalized (solid curve) phases, showing the transition at $T=T'$ of UP for the theoretical model of Table II, column A. The Fermi energy of the band when occupied by one electron per U ion is $\epsilon_0 = 0.444$ eV in this model.

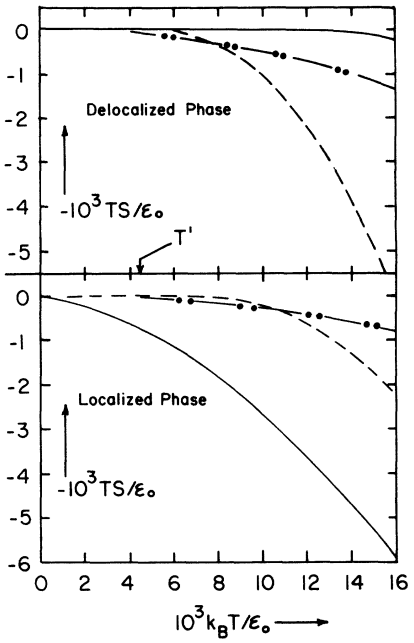

FIG. 10. Theoretical entropy contributions $-TS(T)$ of three types of excitations to the free energy $F=U-TS$ of UP (see Fig. 9) for the delocalized (upper diagram) and localized (lower diagram) phases. The parameters of the calculation are those of Table II, column A. The arrow marks the transition temperature $T'=0.0044\epsilon_0/k_B$, and the Fermi energy of the band when occupied by one electron per U ion is $\epsilon_0=0.444$ eV. Solid curves, excitations of electrons between the band and localized states; dashed curves, magnetic excitations; dash-dotted curves, excitations of electrons within the band.

correctly predicts the change in the magnetic ordering from FM to AFM-I observed at the moment-jump transition of NpC. This may be because the number of conduction electrons w is larger in NpC than in UP, so that the RKKY exchange, which increases (on the average) with w, dominates the direct exchange or superexchange in the former compound, making the RKKY predictions more reliable. The sharp decrease in the occupation of the band as T increases above T' calculated by the three models (Fig. 12) correlates well with the observed rapid increase in the electrical resistivity $\rho(T)$, assuming that the change in $\rho(T)$ is roughly proportional to the change in band occupancy. A more

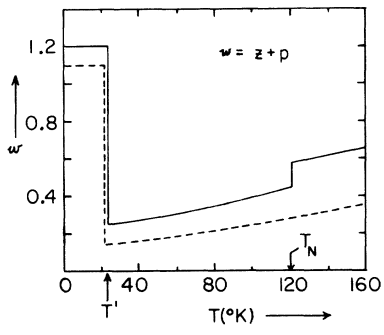

FIG. 11. Theoretical number w of band electrons per uranium ion of UP as a function of temperature T. Dashed curve, present theory with parameters from Table II, column A; solid curve, present theory with parameters from Table II, columns B or C.

TABLE III. Theoretical and experimental values for electronic specific heat coefficient γ and heats of transition H_1 and H_2 of UP. Theories A, B, and C represent three sets of parameters of the electron delocalization model (see also Table II and Figs. 6–11).

	γ(cal/mole °K^2) ($\times 10^{-3}$)	$T'\Delta S$ (cal/mole)	$T_N\Delta S$ (cal/mole)
Experiment	2.30	10.2	87.3
Theory A	2.00	6.5	···
Theory B(or C)	2.46	8.1	87.7

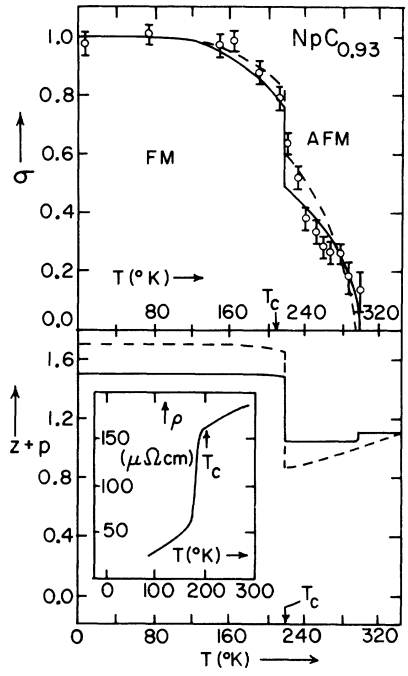

FIG. 12. Relative sublattice magnetization σ (top) and conduction electron number $z+p$ (bottom) per Np-ion as functions of temperature T for $NpC_{0.93}$. $T_c\cong 220$ °K. Top: Circles, experiment of Lander *et al.*, Ref. 4; dashed line, theory with parameters from Table II, columns D or E; solid line, theory with parameters from Table II, column F; Bottom: Dashed line, theory with parameters from Table II, columns D or E; solid line, theory with parameters from Table II, column F: Insert: Specific resistivity vs temperature from experiment of Ref. 8 on another sample, $NpC_{0.96}$, showing the localization transition at $T_c\cong 200$ °K.

quantitative calculation of $\rho(T)$ does not seem justified at this time in view of the unknown contributions of scattering from defect sites, phonons, magnons, and spin fluctuations.

As can be surmised from the decrease in $\sigma(T)$ with increasing T in both the delocalized (FM) and localized AFM-I phases, the entropy of magnetic excitations plays a more important role in the theory of the transition at $T = T'$ in NpC than in the case of UP. There is a more delicate balance between the various components of the free energy, and the simple picture of Sec. II is no longer adequate.

V. DISCUSSION

The electron delocalization model developed herein represents a drastic break from previous theories of the magnetic phase transitions of actinide compounds, in which the actinide ion is assumed to have a well-defined integral number of $5f$ electrons localized on it. By representing the complicated interactions and electronic states of these materials in terms of several phenomenological parameters, we obtain a theory well suited for practical applications. This theory makes it possible to explain the complicated magnetic phase transitions of the metallic actinide compounds within the framework of a single model, as is shown by the applications to UP and NpC presented here and as will be shown in a subsequent paper II by applications to UAs, US, and solid solutions of actinide compounds such as $UP_{1-x}S_x$ and $UAs_{1-x}P_x$. The theory of Sec. III is also directly applicable to materials where the crystal field is negligible so that the ionic configurations i ($i = 0, 1$) are magnetic manifolds of multiplicity $2J_i + 1$ and magnetic moment $\mu_i = \mu_B g_J J_i$. This may describe several rare earth metals and semiconductors such as EuO[51] and $Li_xMn_{1-x}Se$,[52] where the RKKY theory is probably adequate for predicting $J(p)$.

This theory may be critized on the grounds that a large number of parameters are introduced to explain only two curves: the magnetization and susceptibility, and the heats of transition. It should be borne in mind, however, that the large number of parameters enters the theory not because of some *ad hoc* assumptions, but because of the special properties of the actinide compounds. As was already pointed out by Koelling and Freeman,[53] in the actinides, in contrast to the other groups of magnetic elements, several different interactions of the same order of magnitude compete with each other. Each of these interactions is characterized by its own parameters, and it would be entirely unphysical to eliminate some of these parameters for the sake of simplicity.

Although the theory explains the rather complicated magnetization and susceptibility data, its validity may remain questionable due to the large number of parameters referred to above. Also, the values of the parameters listed in Tables II and III are not uniquely determined, because different sets of parameters yield a good fit to the data.

As will be shown in paper II, the same set of parameters as used here provides a good explanation of data on other actinide compounds. In a situation like this, we only hope that the theory will be subjected to further crucial tests in future experiments. For example, the low-temperature electronic specific heat, the heat capacity, and Hall effect measurements on NpC would be very helpful. Similar experiments are currently underway for UAs, USb, and UP.[11] A determination of the effect of an applied magnetic field and of elastic deformation (pressure) on the first-order transitions in the metallic actinide compounds would be interesting, especially if single crystals become available.

A suspicious feature of the theory is that it predicts an electron-delocalization transition; but, as pointed out in Sec. IV A, it is unable to predict whether or not this transition will be accompanied by a volume change of the crystal. Since UP and NpC show no significant volume change, whereas certain rare-earth compounds show such changes when electron delocalization occurs, one may question whether we are dealing with an electron delocalization transition at all in the actinide compounds.

It should be realized that neither the examples citing volume changes at delocalization transitions nor the counter-examples cited in Sec. IV A can decide this question. A decision based on these examples would be tantamount to a conclusion based on analogy, instead of on direct evidence. We feel that the actinides are so different from both iron and rare-earth group compounds that analogies cannot be drawn. The data on resistivity changes as well as the lack of any other quantitatively successful model make us believe that a delocalization transition does indeed occur. We hope that other, direct experimental evidence in the future will decide about the validity of our model.

We plan to extend the theory to include the effects of the hybridization in quantum-mechanically admixing the band and localized states along the lines followed by Anderson.[38] This modification may be necessary to explain the properties of UN, which is thought to show itinerant-electron antiferromagnetism,[8] resulting presumably from strong hybridization and a Fermi level located in the narrow f band. Compared to the other NaCl-type uranium compounds listed in Table I, UN has an anomalously small ordered magnetic moment and a significantly small lattice constant.[32] The former property indicates an effect of strong hybridization and the latter property may be the reason

why the hybridization is stronger in UN than in the other actinide compounds. On the other hand, the neutron-diffraction results,[34] the Curie-Weiss behavior of the paramagnetic susceptibility,[32] and the value ($3.1\mu_B$) of the paramagnetic moment[32] are best explained by the assumption of localized magnetic electrons. Another advantage of considering hybridization is that in principle both long-range and short-range magnetic interactions can be related to the hybridization parameter by a fourth-order perturbation calculation, as has been shown for certain band shapes by da Silva and Falicov.[54]

---

*Work performed in partial fulfillment of the requirements for the Ph.D. degree. Present address: Purdue University, Fort Wayne Campus, 2101 Coliseum Boulevard East, Fort Wayne, Ind. 46805.

[1]P. Erdös and J. M. Robinson, AIP Conf. Proc. **10**, 1070 (1973).

[2]J. F. Counsell *et al.*, Trans. Faraday Soc. **63**, 72 (1967).

[3]S. L. Carr, C. Long, W. G. Moulton, and Moshe Kuznietz, Phys. Rev. Lett. **23**, 786 (1969).

[4]H. H. Lander, L. Heaton, M. G. Mueller, and K. D. Anderson, J. Phys. Chem. Solids **30**, 733 (1969).

[5]L. Heaton *et al.*, J. Phys. Chem. Solids **30**, 453 (1969).

[6]J. Marples, United Kingdom Atomic Energy Agency Report No. AERE-R6279, 1969, Atomic Energy Research Establishment, Harwell, England (unpublished).

[7]J. M. Gulick and W. G. Moulton, Phys. Lett. A **35**, 429 (1971).

[8]M. B. Brodsky, AIP Conf. Proc. **5**, 611 (1972).

[9]G. H. Lander, M. H. Mueller, and J. F. Reddy, Phys. Rev. B **6**, 1880 (1972).

[10]J. Leciejewicz, A. Murasik, and T. Palewski, Phys. Status Solidi B **46**, K67 (1971).

[11]R. Troc (private communication).

[12]Chris Long and Yung-Li Wang, Phys. Rev. B **3**, 1656 (1970).

[13]S. J. Allen, Jr., Phys. Rev. **166**, 530 (1968); Phys. Rev. **167**, 492 (1968).

[14]M. Blume, Phys. Rev. **141**, 517 (1966).

[15]M. A. Kanter and C. W. Kazmierowicz, J. Appl. Phys. **35**, 1053 (1964).

[16]M. Tetenbaum, J. Appl. Phys. **35**, 2468 (1964).

[17]O. L. Kruger and J. B. Moser, J. Chem. Phys. **46**, 891 (1967).

[18]J. F. Counsell, R. M. Dell, and J. F. Martin, Trans. Faraday Soc. **62**, 1736 (1966).

[19]A. J. Arko, M. B. Brodsky, and W. J. Nellis, Phys. Rev. B **5**, 4564 (1972).

[20]B. T. Matthias, discourse, 1970 International Conference on Magnetism, Grenoble, France (unpublished).

[21]J. F. Counsell *et al.*, in *Proceedings of a 1967 Symposium on Thermodynamics of Nuclear Materials* (International Atomic Energy Agency, Vienna, 1968), pp. 385–394.

[22]Z. Fisk and B. R. Coles, J. Phys. C **3**, L104 (1970).

[23]F. A. Wedgwood and M. Kuznietz, J. Phys. C **5**, 3012 (1972).

[24]F. A. Wedgwood, J. Phys. C **5**, 2427 (1972).

[25]H. L. Davis, Nucl. Metall. **17**, 209 (1970), pt. I.

[26]C. Kittel, *Introduction to Solid State Physics*, 3rd ed. (Wiley, New York, 1966).

[27]L. M. Falicov *et al.*, Phys. Rev. Lett. **22**, 297 (1969); Phys. Rev. B **2**, 3383 (1970); Phys. Rev. B **3**, 2425 (1971); Solid State Commun. **10**, 455 (1972).

[28]B. Alascio *et al.*, Phys. Rev. B **5**, 3708 (1972).

[29]J. C. Nickerson *et al.*, Phys. Rev. B **3**, 2030 (1971).

[30]J. Hubbard, Proc. R. Soc. A **285**, 542 (1965).

[31]S. B. Haley and Paul Erdös, Phys. Rev. B **4**, 669 (1971).

[32]J. Grunzweig-Genossar, M. Kuznietz, and F. Friedman, Phys. Rev. **173**, 562 (1968).

[33]C. H. de Novion and R. Lorenzelli, J. Phys. Chem. Solids **29**, 1901 (1968).

[34]N. A. Curry, Proc. Phys. Soc. Lond. **86**, 1193 (1965).

[35]K. R. Lea, M. J. M. Leask, and W. P. Wolf, J. Phys. Chem. Solids **23**, 1381 (1962).

[36]N. A. Curry, Proc. Phys. Soc. Lond. **89**, 427 (1966).

[37]G. H. Lander, M. H. Mueller, and J. F. Reddy, AIP Conf. Proc. **5**, 1371 (1972).

[38]P. W. Anderson, Phys. Rev. **124**, 41 (1961).

[39]R. Jullien, E. Galleani d'Agliano, and B. Coqblin, Phys. Rev. B **6**, 2139 (1972).

[40]L. R. Bickford, Jr., Rev. Mod. Phys. **25**, 75 (1953).

[41]J. Cullen and E. Callen, J. Appl. Phys. **41**, 87 (1970).

[42]D. Adler, Rev. Mod. Phys. **40**, 714 (1968).

[43]V. G. Bhide *et al.*, Phys. Rev. Lett. **28**, 1133 (1972).

[45]M. A. Rudermann and C. Kittel, Phys. Rev. **96**, 99 (1954).

[46]Moshe Kuznietz, G. H. Lander, and Y. Baskin, J. Appl. Phys. **40**, 1130 (1969).

[47]M. Kuznietz, J. Appl. Phys. **42**, 1470 (1971).

[48]M. Kuznietz and J. Grunzweig-Genossar, J. Appl. Phys. **41**, 906 (1970).

[49]J. Leciejewicz, Phys. Status Solidi B **48**, 445 (1971).

[50]D. J. Lam (private communication).

[51]J. B. Torrance *et al.*, Phys. Rev. Lett. **29**, 1168 (1972).

[52]R. R. Heikes, T. R. McGuire, and R. I. Happel, Phys. Rev. **121**, 703 (1961); J. Appl. Phys. **31S**, 276 (1966).

[53]D. D. Koelling and A. J. Freeman, AIP Conf. Proc. **10**, 1300 (1973).

[54]C. E. T. Goncalves da Silva and L. M. Falicov, J. Phys. C **5**, 63 (1972).